Chemical Physics Letters 781 (2021) 138974

Contents lists available at ScienceDirect

Chemical Physics Letters

journal homepage: www.elsevier.com/locate/cplett

Research paper

Polycurcumin nanospheres modified electrode for nanoscale detection of mercury ions in seawater

K. Krishna Kumar [a,b], M. Devendiran [b], R.A. Kalaivani [b], S. Sriman Narayanan [a,*]

[a] Department of Analytical Chemistry, School of Chemical Sciences, University of Madras, Guindy Campus, Chennai, Tamil Nadu 600025, India
[b] Central Instrumentation Laboratory (CIL), Department of Chemistry, School of Basic Science, Vels Institute of Science, Technology and Advanced Studies (VISTAS), Pallavaram, Chennai, Tamil Nadu 600117, India

ARTICLE INFO

Keywords:
Polycurcumin
Electropolymerization
Stripping voltammetry
Mercury ion sensing

ABSTRACT

Curcumin, a β-diketone natural ligand is capable of coordinating and forming a stable complex with a variety of metal ions. In this study, we have reported electropolymerization that can convert macromolecules (curcumin) into nanosphere-shaped polycurcumin film (PCR-NS). The PCR-NS modified electrode was utilized for the detection of Hg^{2+} ions at a nanoscale concentration by the differential pulse anodic stripping voltammetry (DPASV) technique. Surface morphology and electrochemical behavior of the PCR-NS electrode and its metal complex were characterized. Parameters such as the effect of electrolyte, pH, preconcentration time were optimized for selective determination of Hg^{2+} ions with the linear concentration range from 0.21 to 21.72 μgL^{-1}, with LOD 70.49 ngL^{-1}.

1. Introduction

The alarming increase in heavy metal-related toxicity has become a major environmental crisis [1]. Heavy metals such as lead, mercury, and cadmium pose threat to several life forms in both land and water bodies [2]. Several analytical methods such as Atomic Absorption Spectroscopy (AAS) [3], Inductively Coupled Plasma Mass Spectrometry (ICP-MS) [4], have been employed for the determination of trace levels of metal contaminations in environmental samples but these methods suffer from many disadvantages such as poor time efficiency, skilled technicians, sophisticated facilities and tedious sample preparation, which make them unsuitable for continuous assessment. Nanomaterials such as gold micro shells [5], ZnO/Ag nanoarray [6], and gold-coated TiO_2 nanotube array [7] were employed for removal and sensing of organic and inorganic pollutants using Surface Enhanced Raman Spectroscopy (SERS) technique. Electroanalytical techniques can be considered as an alternative for the conventional methods [8,9] where stripping voltammetry has been commonly employed for the determination of metal ions and toxins in food samples [10]. In conventional voltammetric techniques, mercury-based electrodes have been extensively used as working electrodes for the determination of heavy metals due to their amalgam forming property [11], but they have a disadvantage as mercury is toxic [12]. To overcome this demerit, over the past two decades mercury-free electrodes have been emerging for metal ion sensing [13]. In our previous work, we have reported mercury-free electrode using metallochromic indicators namely poly xylenol orange [14], poly O-cresophthalein [15], and poly zincon [16] for the determination of metal (II) ions. The utilization of biological compounds as chelating agents has also become a suitable option for heavy metal detection as they are inexpensive, non-toxic, and eco-friendly [17]. Curcumin (CR), (1,7-bis (4-hydroxy-3-methoxyphenyl)-1,6-heptadinene-3,5-dione) is the principal compound of curcuminoids which is extracted from the rhizome of the Indian perennial herb *Curcuma longa*[18]. The β-diketo functionality and unsaturated phenolic group of curcumin structure form homoleptic complexation with most of the metal ions [19]. Several studies have been conducted using Ni (II)-curcumin complexes as a chemical sensor for the determination of analytes such methanol [20], amino acids [21], fructose [22], and amoxicillin [23]. Curcumin functionalized gold nanoparticles have enhanced the electrocatalytic property of curcumin towards the determination of dopamine [24]. A chemosensor method for the determination of mercury was developed using curcumin nanoparticles for the microscale sensing of Hg^{2+} ions [25]. Curcumin (CR) was first applied for the electrochemical determination of anions and cations using a curcumin-MnO_2-Graphene nanosheet modified glassy

* Corresponding author at: Department of Analytical Chemistry, University of Madras, Guindy campus, Chennai, Tamil Nadu 600025, India.
E-mail addresses: krishnakumar260888@hotmail.com (K. Krishna Kumar), chemist.deva@gmail.com (M. Devendiran), director.sbs@velsuniv.ac.in (R.A. Kalaivani), sriman55@yahoo.com (S. Sriman Narayanan).

https://doi.org/10.1016/j.cplett.2021.138974
Received 8 May 2020; Received in revised form 11 August 2021; Accepted 12 August 2021
Available online 13 August 2021
0009-2614/

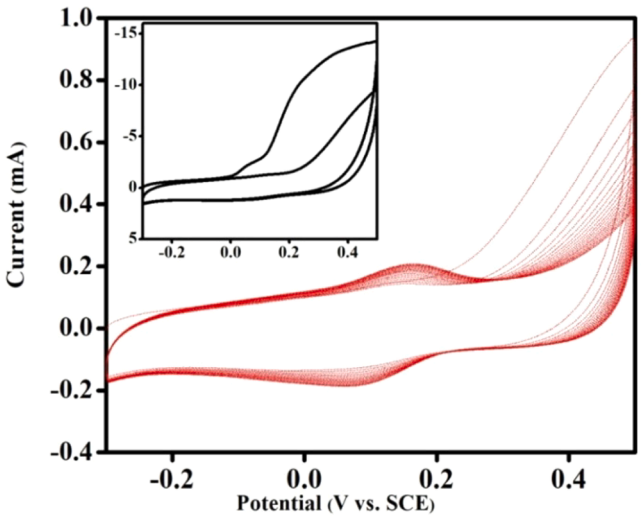

Fig. 1. CVs obtained during electropolymerization of curcumin on bare electrode in 0.1 M phosphate buffer solution of pH 7 at 50 mVs^{-1}. **(Inset)** CVs of first two cycles of electropolymerization.

carbon electrode [26]. But due to the unstable nature of curcumin on the electrode surface, electropolymerization fabrication was found to be an alternative to develop a stable curcumin-based electrode. A recent study has developed a dual electrochemical and fluorescent assay using electropolymerized curcumin-graphene quantum dots modified indium tin oxide electrode for determination of Apo e4 allele gene [27]. K.M. Mohibul Kabir, et al, reported nanosphere-shaped gold nanoparticles for microscale detection of elemental mercury using a quartz crystal microbalance device [28].

Among all other heavy metals, mercury was more prevalent in water contamination from industrial effluents such as mining plants, energy, etc. [6]. In the present study, curcumin was electropolymerized on the electrode material as polycurcumin film and applied to preconcentration and differential pulse anodic stripping voltammetry (DPASV) sensing of Hg^{2+} ions. The electrochemically fabricated polycurcumin molecules appeared as a nanosphere (approximately 250 nm in size) and decorated on the electrode surface. Polycurcumin in general has the property of electrocatalysis**.** Polycurcumin (PCR) based electrodes have been developed and used as chemical sensors [29]. Herein for the first time, we have developed an analytical method using polycurucmin nanosphere (PCR-NS) modified electrode for trace level determination of Hg^{2+} ions. Parameters and experimental conditions for the detection of individual Hg^{2+} ions using PCR-NS modified electrodes were optimized and applied for real sample analysis.

2. Experimental methodology

2.1. Chemicals and reagents

A graphite rod (Length- 150 mm, Diameter- 3 mm) was purchased from Sigma-Aldrich. Curcumin and AAS standard solutions of cadmium (Cd), lead (Pb), mercury (Hg), zinc (Zn), and copper (Cu) were obtained from SRL, India. All other chemicals used in this study were from Merck. All aqueous reagents used in this experiment were prepared using double distilled water (conductivity- 0.8–1.2 μS/cm).

2.2. Instrumentation

The distilled water was prepared using a double stage distillation unit horizontal model (Rivera Glass private limited, India). Electrochemical experiments such as cyclic voltammetry (CV), chronoamperometry, differential pulse stripping voltammetry (DPASV) were carried out in an electrochemical workstation, (CH Instruments, USA, Model- 660B) using a conventional three-electrode cell with standard calomel electrode (SCE) as reference electrode, platinum electrode as an auxiliary electrode and PCR-NS modified electrode as the working electrode. Attenuated total reflectance- Fourier transform infrared (ATR-FTIR) spectra for PCR-NS modified electrode and metal preconcentrated PCR-NS modified electrode was recorded using FTIR spectrometer (PerkinElmer, USA, Model- Spectrum 2 UATR). Surface morphology of PCR-NS and metal preconcentrated PCR-NS modified electrode was performed using a scanning electron microscope (SEM) (TESCAN, USA, Model- VEGA3) with an accelerating voltage of 30 kV. The elemental analysis and color mapping were carried out using energy dispersive X-ray analysis (Bruker Nano, Germany). The results obtained by the developed method for the trace level determination of metal ions in seawater were compared with AAS (PerkinElmer, USA, Model- AA-800). All the experiments were carried out under ambient conditions.

2.3. Preparation of polycurcumin nanosphere film electrode

The paraffin wax impregnated graphite rods used as a bare electrode for modification were subjected to pretreatment before electropolymerization of curcumin. To remove the impurities present, graphite electrodes were washed with acetone, ethanol, and water followed by impregnation with paraffin wax [30]**.** The paraffin wax impregnated graphite (PIG) electrodes were polished using 350 μm and then with 1000 μm SiC coated abrasive papers. The electrode surface was then smoothened to mirror finish by polishing with alumina slurry of different micron sizes (1, 0.3, and 0.05) and then washed with double distilled water. Modification of the bare electrode with curcumin was carried out as reported earlier [21]**.** Briefly, 10 μL of ethanolic solution of curcumin (25 mM) was drop casted on the surface of the bare electrode followed by drying under vacuum. After drying, curcumin was electropolymerized in 0.1 M phosphate buffer (pH 7) with 20 continuous cycles from −0.3 V to 0.8 V at the scan rate of 50 mV s^{-1} to obtain PCR-NS modified electrode.

2.4. Determination of Hg^{2+} with PCR-NS modified electrode using DPASV

Several steps are involved for the DPASV determination of Hg^{2+} using PCR-NS modified electrode. Following are the pre-concentration time, reduction potential, stripping analysis, and surface regeneration procedures described the same was portrayed in the graphical abstract.

Step-1: The PCR-NS modified electrode was dipped in 0.1 M NH_4NO_3 containing Hg^{2+} ions and preconcentrated for 300 sec under stirring condition

$$Hg^{2+}_{(aq)} + PCR\text{ - }NS_{(s)} \xrightarrow[300\ sec]{300\ rpm} \left[Hg^{2+}_{-}PCR\text{ - }NS\right]_{(s)}$$

Step-2: Hg^{2+} preconcentrated PCR-NS modified electrode was transferred to a fresh 0.1 M NH_4NO_3 of pH 5.5 and potential of −0.1 V was applied for 60 sec to reduce Hg^{2+} to Hg^0.

$$Hg^{2+}_{-}PCR\text{ - }NS_{(s)} \xrightarrow[+2e]{-0.10\ V,60\ sec} \left[Hg^{0}_{-}\ PCR\text{ - }NS\right]_{(s)}$$

Step-3: DPASV was carried out by scanning the potential from −0.3 V to 0.8 V with a pulse amplitude of 50 mV and a pulse width of 5 sec. The stripping current for the Hg^{2+} was measured at a potential of +0.2 V.

$$Hg^{0}_{-}\ PCR\text{ - }NS_{(s)} \xrightarrow[-2e]{DPASV-0.3\ to\ +\ 0.8\ V} \left[Hg^{2+}_{-}\ PCR\text{ - }NS\right]_{(s)}$$

Step-4: After completing the experiment, the electrode surface was renewed by applying the potential from 0 to +1.2 V followed by dipping the electrode in 50 mM EDTA solution for 300 sec.

$$Hg^{2+}_{-}PCR\text{ - }NS_{(s)} \xrightarrow[300\ sec]{50\ mM\ EDTA} EDTA\text{ - }Hg^{2+}_{(aq)} + PCR\text{ - }NS_{(s)}$$

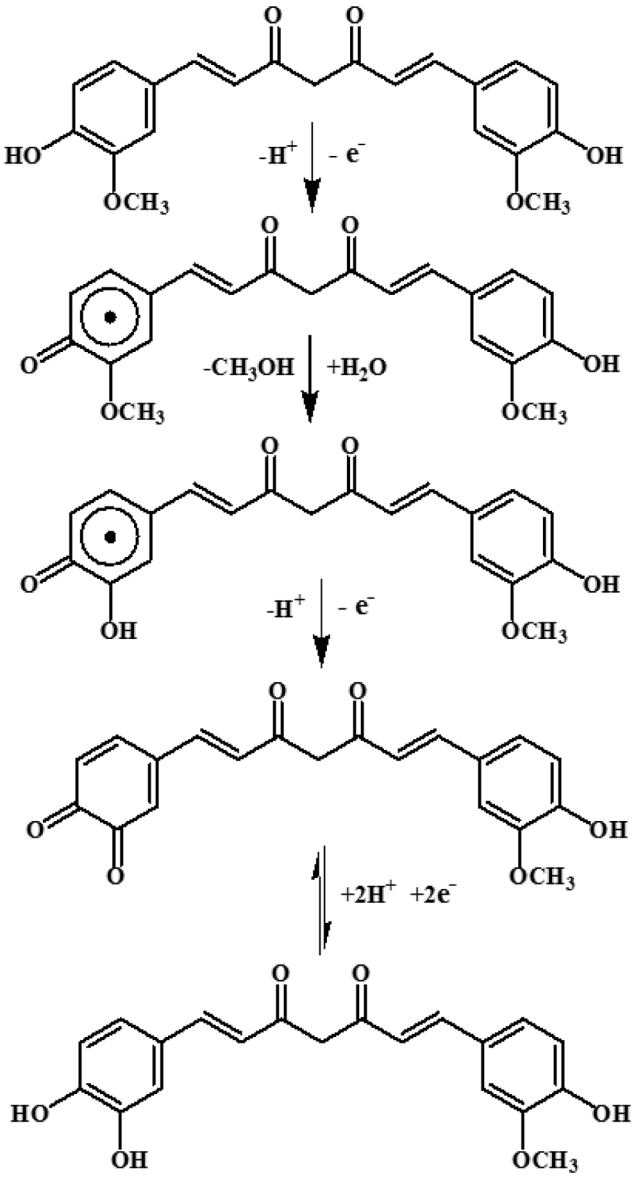

Scheme 1. Electropolymerization and redox mechanism of polycurcumin film modified electrode.

2.5. Preparation of sea water sample

For the real sample analysis, the sea water was collected from Marina Beach, Chennai, India and filtered using Whatman filter paper Grade 1. The sea water was spiked with three replication of AAS grade Hg^{2+} ions solution to obtain 0.101 μgL^{-1} concentration and the PCR-NS modified electrode was preconcentrated for 300 sec. The Hg^{2+}-PCR-NS electrode was transferred into the 0.1 M NH_4NO_3 of pH 5.5 and −0.1 V reduction potential was applied for 60 sec and DPASV analysis was performed under optimized condition.

3. Results and discussion

3.1. Electro polymerization mechanism

The cyclic voltammograms during the electropolymerization of curcumin were shown in Fig. 1. Curcumin was electropolymerized on the working electrode surface by scanning the potential from −0.3 to + 0.6 V at a scan rate of 50 mVs^{-1} for 20 cycles in 0.1 M phosphate buffer solution (pH 7). The CVs for the first two cycles of electropolymerization were shown in **inset** Fig. 1**,** where the initial oxidation of curcumin begins at the potential of + 0.15 V and extended to the potential to + 0.4 V. The phenolic group of curcumin contributed to the initial oxidation, where the phenolic group was converted into phenolate ion. During the reverse scan, a cathodic peak corresponding to the reduction of curcumin (E_{pc}) appeared at + 0.09 V. In this process the methoxy group of curcumin was eliminated as methanol by hydrolysis, giving away the anion leading to the formation of highly reactive *O*-quinone [29]. Following further segments of the CV scan showed stable oxidation and reduction peak for polycurcumin at + 0.18 V and + 0.09 V, respectively. As the potential scan from −0.3 to 0.6 V was continued for 20 cycles, the anodic **(i_{pa})** and cathodic **(i_{pc})** peak currents gradually increased, then the peak current reached saturation indicating that the formation of electropolymerized polycurcumin film on the electrode surface. After electropolymerization, the PCR-NS film modified electrode was rinsed with double distilled water, dried, and employed for metal ion determination. Replicates of PCR-NS modified electrodes were prepared with a similar procedure for characterization. Scheme. 1 represents the structural elucidation for the formation of polycurcumin film and its redox behavior.

3.2. Electrochemical characterization of bare and PCR-NS modified electrode

CV study was carried out to compare the electrochemical behavior of bare and PCR-NS modified electrode. Cyclic voltammetry was employed by applying the potential from −0.3 to + 0.8 V in 0.1 M phosphate buffer solution (pH 7) at a scan rate of 50 mVs^{-1}. Fig. 2 **(i)** shows the CVs of **(a)** bare electrode and **(b)** PCR-NS modified electrode. The unmodified electrode **(curve a)** shows a low background current for both forward and reverse scans without any significant redox peaks. But the PCR-NS modified electrode, **(curve b)** exhibited well-defined redox peaks at the potentials (E_{pa}) + 0.26 V, and (E_{pc}) + 0.16 V at a ΔEp of 100 mV. The redox process in PCR-NS modified electrodes was said to be quasi-reversible as the cathodic and anodic potential difference ($\Delta E_p = |E_{pa} - E_{pc}|$) for this electrode was around 100 mV/n, which was expected to be greater than 56.5 mV/n for a standard reversible system [31]**.** In Fig. 2**,** the background current of the PCR-NS modified electrode **(curve b)** was higher compared to an unmodified electrode **(curve a)**.

The electrochemical property of **(a)** bare PIG electrode and **(b)** PCR-NS film-coated PIG electrode in the presence of standard redox probe $Fe(CN)_6^{3-/4-}$ (5.0×10^{-3} M of $Fe(CN)_6^{3-/4-}$ in 0.1 M of KCl solution) which was characterized using CV (Fig. 2 **(ii))** and electrochemical impedance spectroscopy (EIS) techniques (Fig. 2 **(iii)).** The CV results showed that when compared with a bare electrode, the PCR-NS modified electrode is electrochemically active and could facilitate a reversible electron transfer process. At the higher-frequency region, the Nyquist plot of EIS also showed a bigger semi-circle for bare electrode compared with PCR-NS modified electrode. This is due to the existence of impedance because of the higher potential charge rate for a bare electrode. Thus PCR-NS electrode was used for developing an electrochemical sensor for the determination of Hg^{2+} ions.

3.3. Surface morphological studies of PCR-NS modified electrode

The changes that occurred in the surface of the working electrode during electropolymerization of curcumin were analyzed using FE-SEM. Curcumin was drop casted on the working surface of the graphite electrode and an FE-SEM image was recorded. Fig. 3 shows the FE-SEM image of curcumin drop casted on an electrode **(i)** before electropolymerization and **(ii)** after electropolymerization. The presence of evenly distributed monomers of curcumin molecules was found on the electrode surface (Fig. 3**. (a)).** The appearance of less number of micron size, sphere-shaped CR was due to physical adsorption of monomers at the surface-active sites of the bare electrode. However, after performing

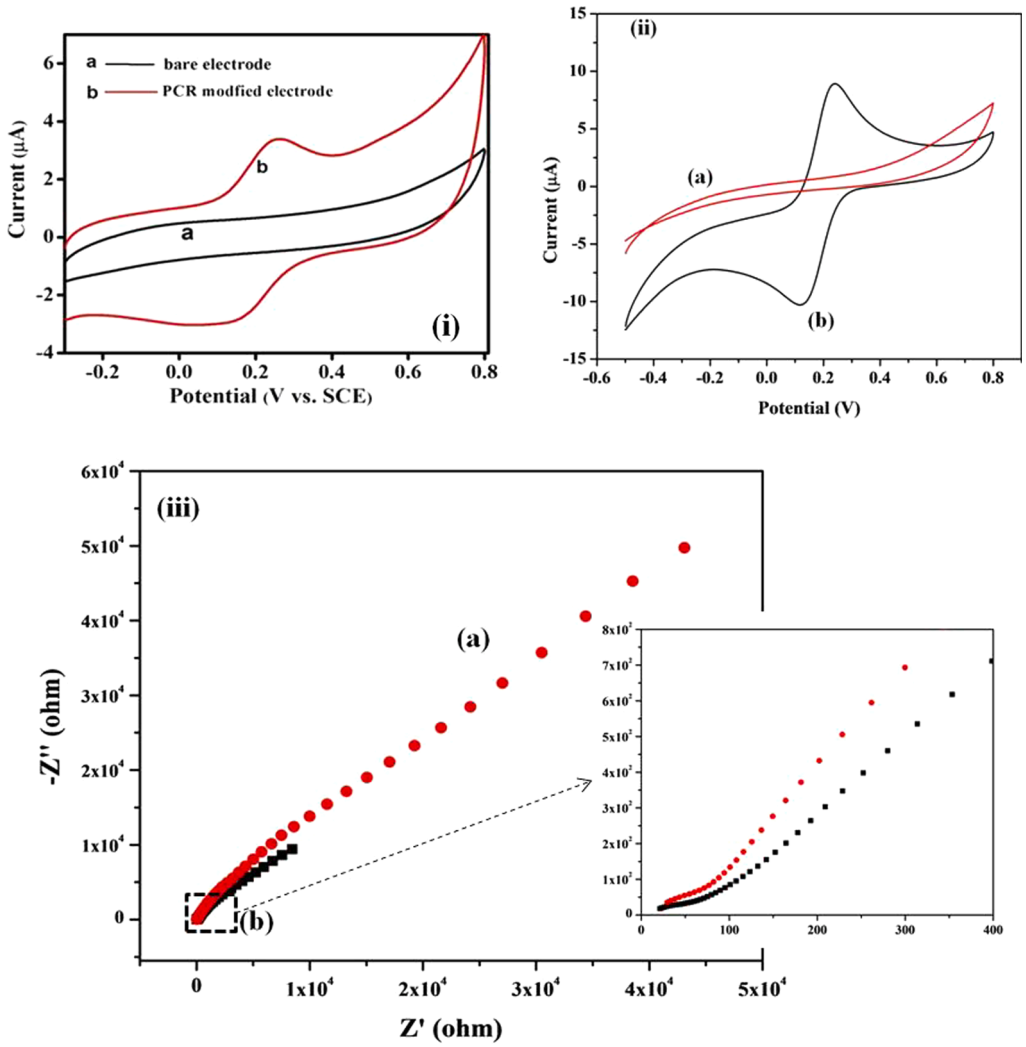

Fig. 2. Cyclic voltammograms for **(a)** bare and **(b)** PCR-NS modified electrode **(i)** in 0.1 M phosphate buffer solution at pH 7. **(ii)** in 0.1 M of KCl containing 0.005 M containing $Fe(CN)_6^{3-/4-}$; scan rate at 50 mVs^{-1}. (iii) corresponding EIS spectra.

20 cycles of CV measurement, the micron size CR molecules conjugated and formed as elongated structures with branched chains resulting in the formation of several nanospheres shaped polymeric film coating with an average particle size of 250 nm in diameter over the electrode surface **(**Fig. 3**.(b)).** As the potential applied during electropolymerization increased the number of radicals, in turn, increased the monomer concentration and exhibited multiple nanospheres on the electrode surface. B. Devadas et al [24] reported the rod-shaped morphology for polycurcumin on electrochemically activated glassy carbon (GC) electrodes. In this report [24], the electropolymerization of curcumin present in 0.1 M phosphate buffer pH 8 solutions was performed using the cyclic voltammetry technique. Electro polymerization in alkali pH may lead to a change in the morphology of PCR into a rod shape. Also, at this condition polycurcumin exhibit enol-form which is not suitable for metal complexation. The present work reported the formation of nanosphere-shaped morphology for polycurcumin on the PIG electrode surface. Since curcumin is insoluble in water or buffer with pH $\leq$ 7.5, in the present work; ethanolic solution of curcumin was drop casted on the PIG electrode surface. The electropolymerization was performed using the CV technique by dipping curcumin drop casted PIG electrode in 0.1 M phosphate buffer, pH 7 solution. At this condition polycurcumin exhibits β-diketo-form which is suitable for metal complexation.

The elemental survey spectrum and color mapping for the PCR-NS modified electrode to calculate the atomic percentage and binding energy were recorded using EDS analysis. Fig. 3 represents **(i)** the carbon atoms in brown color, **(ii)** the oxygen atoms in green color, and **(iii)** the merged image of both **(i)** and **(ii).** The EDS spectra (Figure 4 **(iv))** confirmed the presence of both the atoms with the atomic percentage of carbon at 95.54% and oxygen at 4.46% **(inset table)** which proves that the PCR-NS modified electrode surface was free from contaminations.

3.4. Characterization of metal preconcentrated PCR-NS modified electrode

The Physico-chemical properties of the PCR-NS modified electrode changed during their interaction with metal ions. Comparison of the bare and modified electrode before and after preconcentration with Hg^{2+} ions were characterized to understand the surface behavior of both the electrodes. The following section illustrates the chemical, morphological and electrochemical behavior of modified electrode and its metal complex

3.4.1. ATR-FTIR characterization

The functional groups present at the surface of PCR-NS modified electrodes were measured using IR spectroscopy. The ATR-FTIR spectrum for PCR-NS modified electrodes was acquired from 3600 to 400 cm^{-1}. The IR spectrum (Figure 4 **(a))** shows well-defined peaks at 2360 cm^{-1}, 2845 cm^{-1}, 2915 cm^{-1}, 3511 cm^{-1} corresponding to the hydroxyl

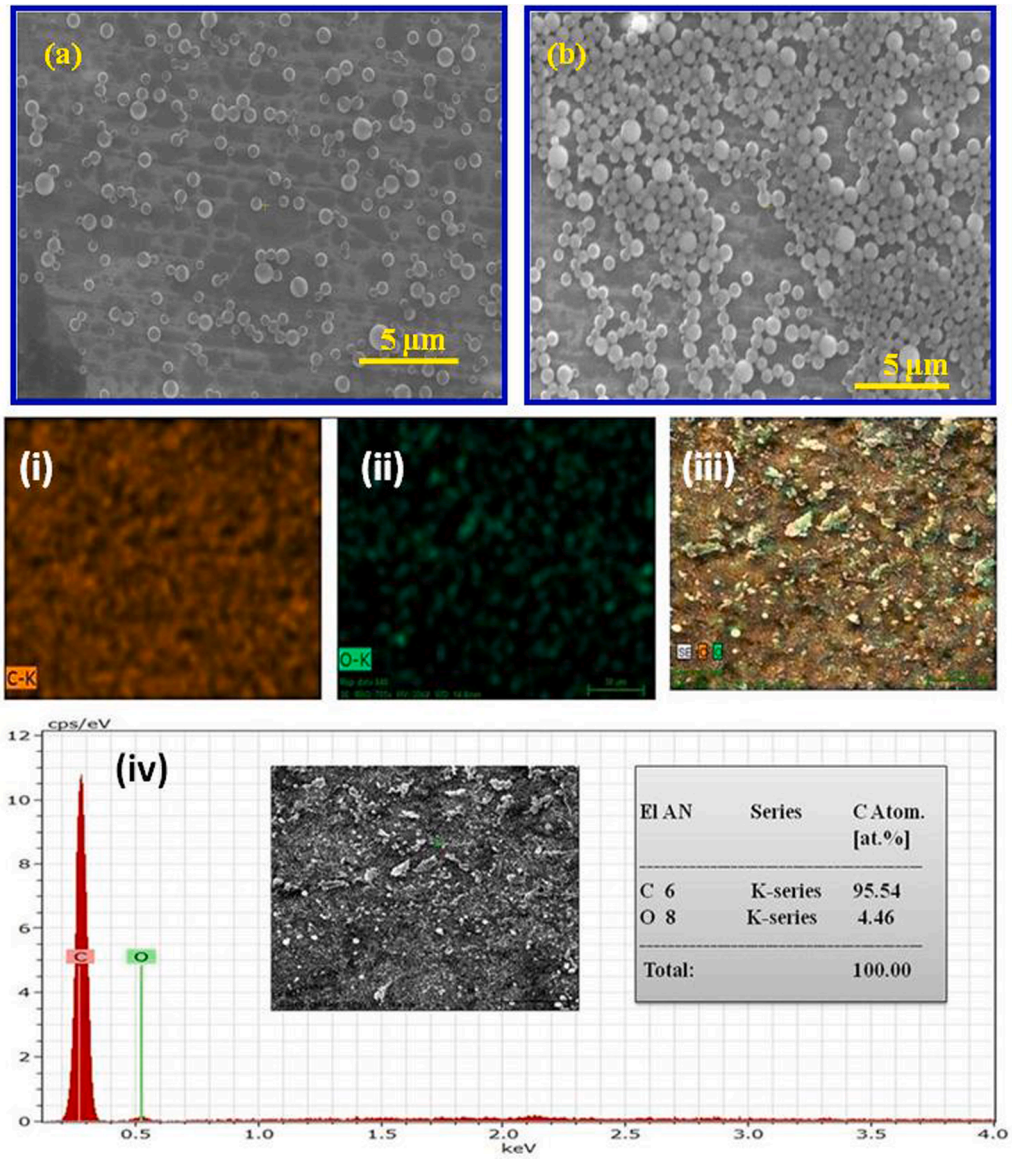

Fig. 3. SEM image of CR drop casted electrode **(a)** before electropolymerization and **(b)** after 20 cycles Elemental color mapping image of PCR-NS modified electrode **(i)** C, **(ii)** O, **(iii)** C,O and **(iv)** respective EDS spectra **(inset)** SEM image of PCR modified electrode and elemental table with atomic percentage.

and methoxy groups of a phenyl ring of polycurcumin [32]. The peaks at 1027, 844 cm^{-1} corresponds to the C–O–C stretching vibrations, 1263 cm^{-1} was for aromatic C–O stretching vibrations, and 1427 cm^{-1} was for olefinic C-H bending vibrations. For the bending vibrations of aliphatic groups (δ CC-C, δ CC = O) peak appeared at 1507 cm^{-1} and the stretching vibration for the aromatic ring appeared at 1568 cm^{-1}. The stretching vibrations for alkenes (C = C) and carbonyl (C = O) groups appeared at 1630 cm^{-1} [33]. The ATR-FTIR results of the PCR-NS modified electrode confirmed that all the functional groups obtained corresponds to the electropolymerized film of curcumin.

For IR spectrum of Hg^{2+} preconcentrated PCR-NS modified electrode showed variation in the intensity of major peaks and shift in the minor peaks **(**Figure 4 **(b))**. At the region 1507 cm^{-1} a peak corresponding to the δ CC-C, δ CC = O of PCR–NS was found to have less intensity after Hg^{2+} preconcentration. Additionally, the intense peak at 2845 cm^{-1} and 2915 cm^{-1} corresponding to the hydroxyl and methoxy groups of the phenyl ring of PCR also increased. Also the peaks at 1027 and 844 cm^{-1} for C–O–C stretching vibrations shifted as a single peak to the region 1046 cm^{-1}. A peak at 1263 cm^{-1} corresponding to aromatic C–O stretching vibrations, and 1427 $cm^{-1}$for olefinic C-H bending vibrations exhibited a slight shift in the peak towards 1284 cm^{-1} and 1466 cm^{-1}, respectively. From the FTIR analysis, it was attributed that major changes in C–O bonds were due to PCR-NS by donating the ion pair electron of oxygen atom and form complex with Hg^{2+} ions [32].

3.4.2. *SEM-EDS studies*

The SEM morphology shown in Fig. 5 was obtained for Hg^{2+} preconcentrated PCR-NS modified electrode which was recorded in different magnifications, and scale bar at **[a] 4 kX,** 10 µm **[b, c] , 6 kX,** 5 µm, and **[d, c, f] , 11 kX,** 2 µm. For SEM analysis, the Hg^{2+} preconcentrated PCR-NS modified electrode was prepared under the optimized condition as discussed in section 2.4 and the samples were examined at 30 kV acceleration voltage. From the SEM results it can be observed that after preconcentration of 3.9×10^{-6} gL^{-1} of Hg^{2+} ions over PCR-NS electrode, the surface appeared as clusters of aggregated Hg^{2+} particles conjugated with polycurcumin. The change in the morphology was due to a change in a polymorph of polycurcumin after complexing with Hg^{2+} ions. Supporting the SEM results the EDS analysis also confirmed the presence of Hg^{2+}. The elemental composition of the Hg^{2+} preconcentrated PCR-NS modified electrode was evaluated by color

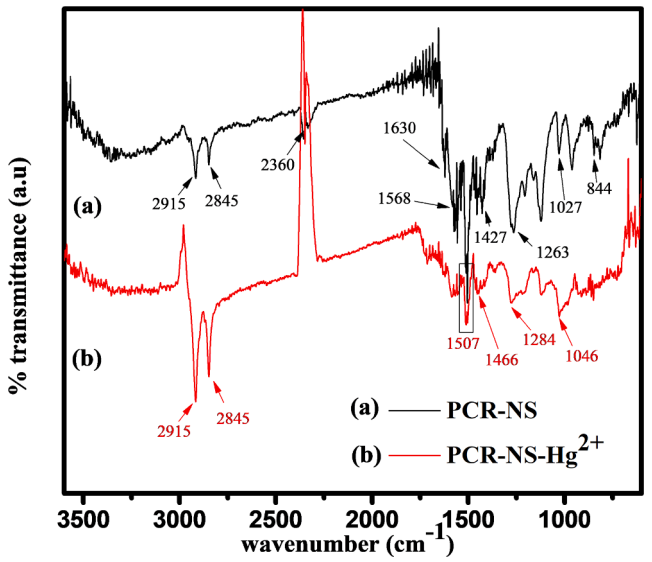

Fig. 4. ATR-IR spectra for PCR-NS modified electrode **(a)** and. PCR-NS-Hg (II) modified electrode **(b)**.

mapping. The major element present on the surface of the electrode is carbon which is depicted in brown-green color **(i)** with an atomic percentage of 75.52% **(inset table).** After carbon, oxygen was the next major component which is represented in pink color **(ii)** with an atomic percentage of 20.21%. Trace amounts of mercury were represented in blue color with an atomic percentage of 0.33%. Additional elements present in the EDS spectra are due to the interference of anions present in the background electrolyte.

3.4.3. *Electrochemical characterization of Hg^{2+}-PCR-NS modified electrode*

Fig. 6 shows the CV curves recorded for **(i)** bare and **(ii)** PCR-NS modified electrodes in the **(a)** absence and **(b)** presence of Hg^{2+} ions. The CV measurement was carried out starting from the potential −0.3 to 0.8 V. The CV curve recorded for the bare electrode without preconcentration of Hg^{2+} ions **(curve a in** Fig. 6(i)**)** does not show any significant peaks corresponding to mercury. But the bare electrode subjected to preconcentration with 3.9×10^{-6} gL^{-1} of Hg^{2+} ions present in 0.1 M NH_4NO_3 electrolyte solution **(curve b in** Fig. 6(i)**)** showed a well-defined oxidation peak for Hg^{2+} at + 0.22 V. The presence of Hg^{2+} ions at the surface of the bare electrode is due to physisorption phenomena. Graphitic carbon tends to adsorb metal to its active surface, whereas the PCR-NS modified electrode forms chemical coordination with Hg^{2+} ions. The CV was performed for PCR-NS modified electrodes without Hg^{2+} ions **(curve a in** Fig. 6**(ii))** which showed redox peak E_{pa} at + 0.42 V and E_{pc} at + 0.32 V. The PCR-NS modified electrode preconcentrated with Hg^{2+} ions **(curve b in** Fig. 6**.(ii))** showed two oxidation peaks at + 0.20 V corresponding to the oxidation of Hg^0 and at + 0.52 V corresponding to the oxidation of Hg^{2+}-PCR-NS. The cathodic scan showed a single reduction peak at + 0.45 V corresponding to the Hg^0-PCR-NS complex. Compared with the PCR-NS modified electrode, the Hg^{2+} ion preconcentrated PCR-NS modified electrode showed significant changes such as a shift in redox peak of PCR-NS and increase in peak current intensity after preconcentration with Hg^{2+} ions. The shift in the redox peak was due to metal complex formation. A

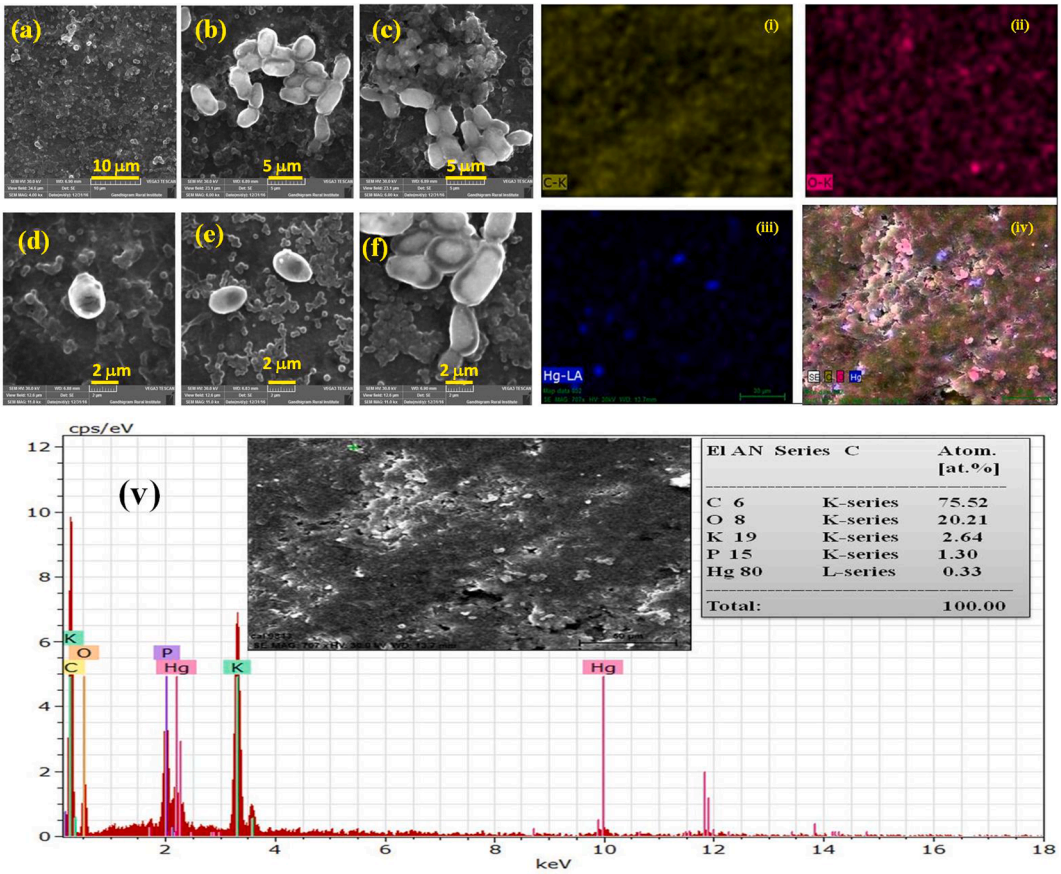

Fig. 5. FESEM image of Hg (II)-PCR–NS modified electrode at different scale bar magnification **[a]** 10 µm **[b, c]** 5 µm, and **[d, e, f]** 2 µM size magnified images. Elemental colour mapping of Hg (II)-PCR-NS electrode, **(i)** carbon, **(ii)** oxygen, **(iii)** Mercury, **(iv)** overall elements **(C, O, Hg)**, and **(v)** EDS spectra **(inset)** SEM image with table of elements present and its atomic percentage.

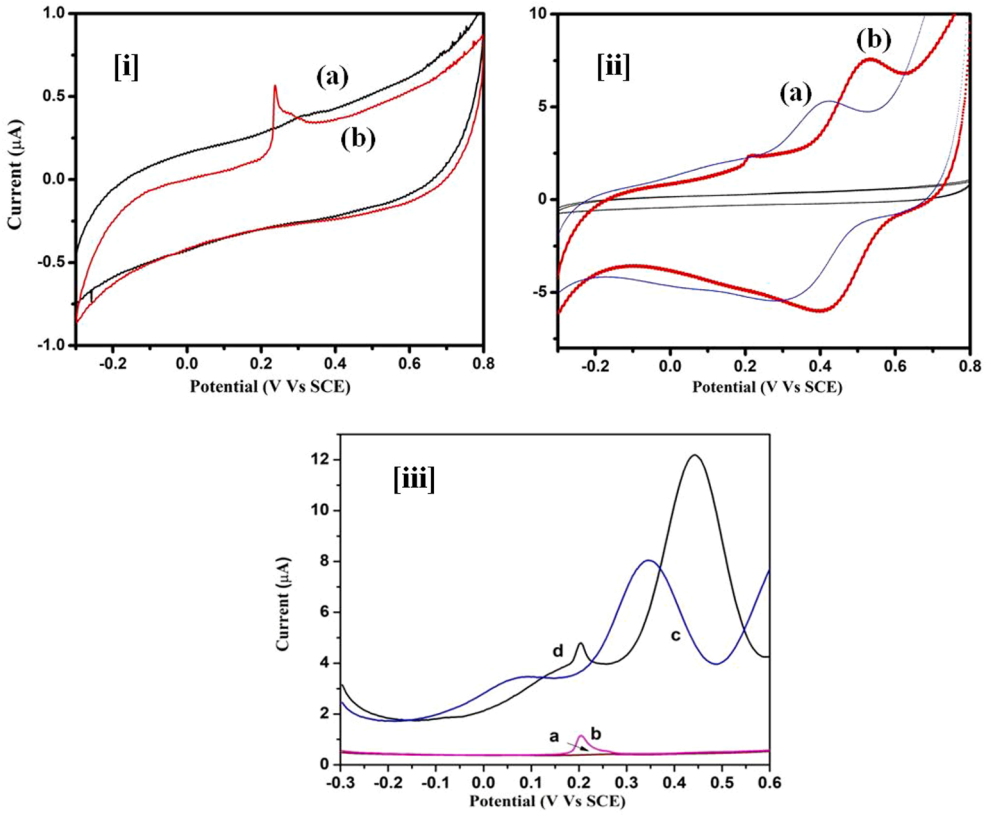

Fig. 6. CV carried out at the scan rate 50 mVs^{-1} for **(i)** bare electrode, and **(ii)** PC-NS modified electrode, **(a)** without and **(b)** with Hg (II) ions pre-concentration. **(iii)** DPASV response of bare electrode **(a)** without and **(b)** with Hg (II) ions pre-concentration, PCR-NS modified electrode **(c)** without and **(d)** with Hg (II) ions pre-concentration. Background electrolyte (0.1 M) NH_4NO_3 containing 3.9×10^{-6} $gL^{-1}$of Hg (II), anodic striping scan between −0.3 to 0.8 V.

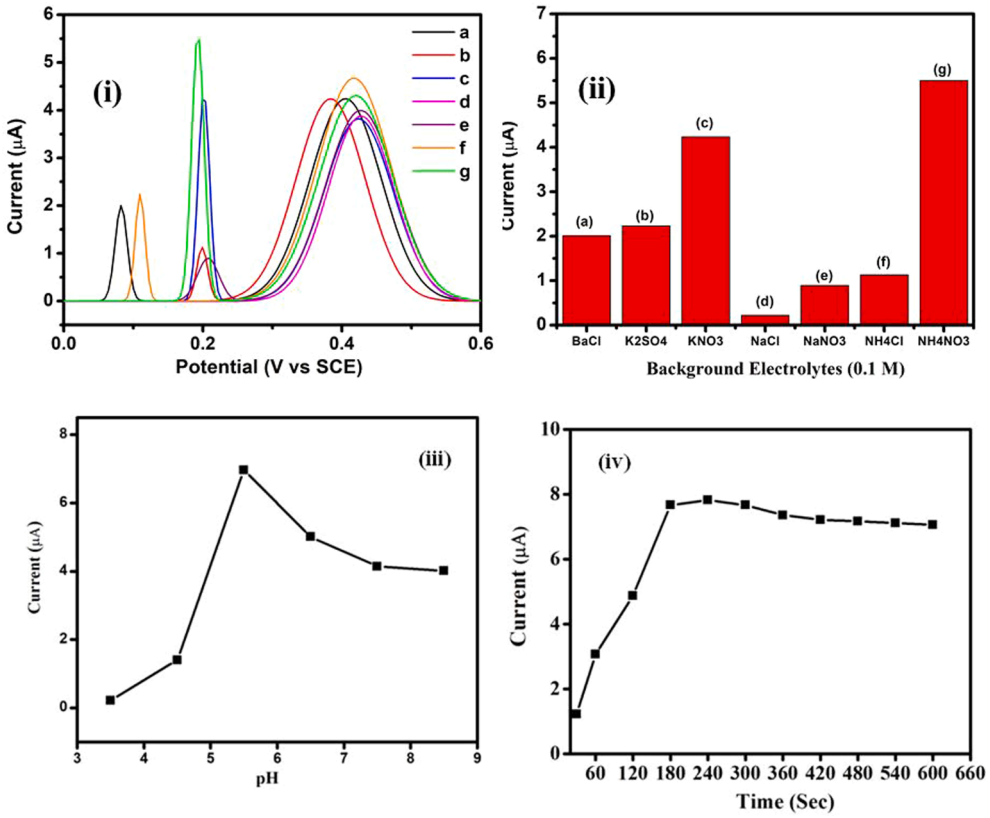

Fig. 7. (i) DPASV response of PCR-NS modified electrode at different background electrolyte (0.1 M) containing Hg (II), anodic striping scan between −0.3 to 0.8 V. **(ii)** corresponding bar chart for peak current versus different background electrolyte. **(iii)** A graph plot corresponding to the stripping signal recorded for Hg (0)- PCR-NS modified electrode versus different electrolyte pH and **(iv)** graph plot corresponding to the strupping signal recorded for Hg(0)- PCR-NS modified electrode versus preconcentration time.

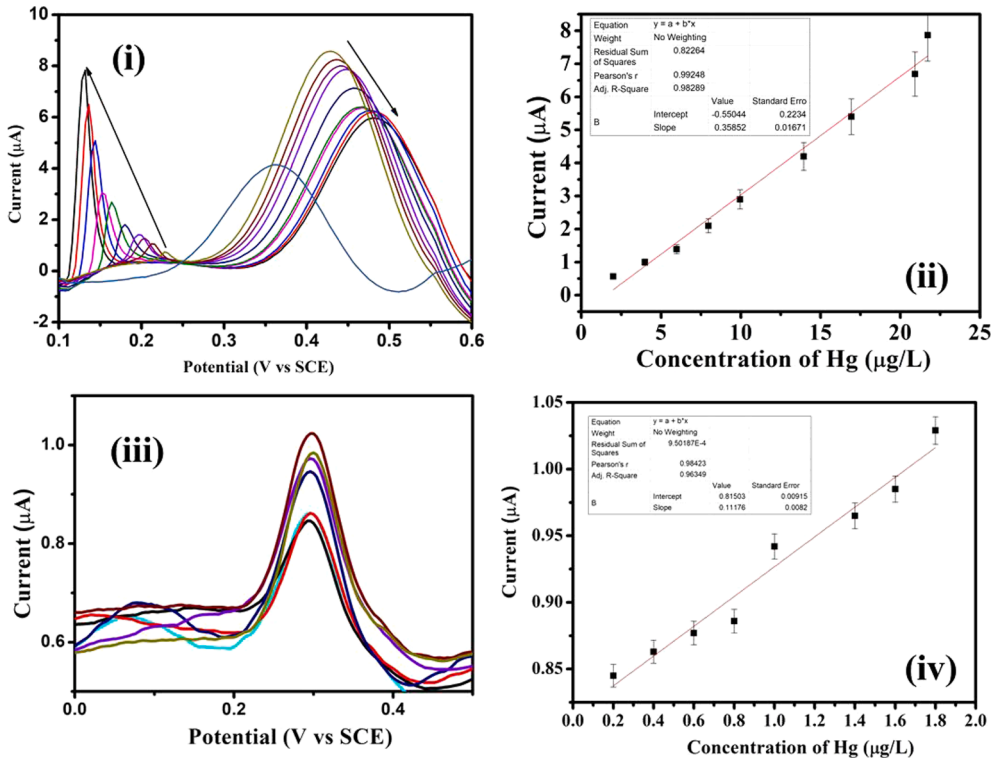

Fig. 8. **(i)** Higher concentration and **(iii)** lower concentration (0.21 to 21.72 μgL^{-1}), DPASV response for Hg(0)-PCR-NS modified electrode in 0.1 M, stripping scan between −0.1 to 0.8 V. **(ii)** and **(iv)** corresponding linear graph.

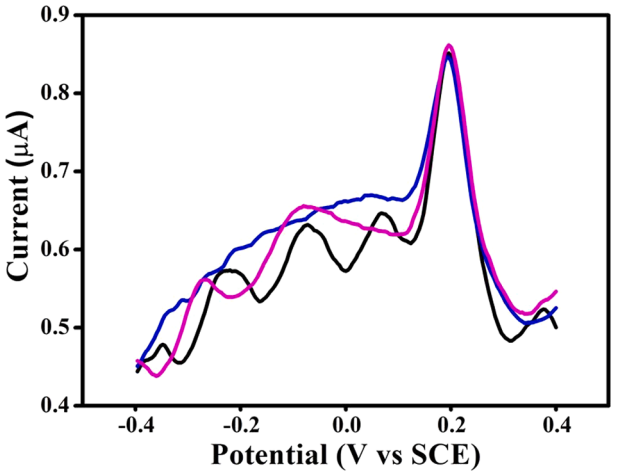

Fig. 9. DPASV curve for PCR-NS electrode after preconcentrated in seawater spiked with (0.1 μgL^{-1}) Hg^{2+} of AAS standard solution.

Table.1
Comparison of Real sample analysis of Hg^{2+} content between present method and atomic absorption spectroscopy.

Real Sample	Hg^{2+} AAS standard solution	DPASV at + 0.1 V (Present Method)		Atomic Absorption Spectroscopy at 253.7 (nm)	
Sea water	Added (mg/L)	Found (mg/L)	Recovery (%)	Found (mg/L)	Recovery (%)
R1	0.101	0.101	100	0.100	99.00
R2	0.102	0.101	99.01	0.100	98.03
R3	0.105	0.104	99.04	0.105	100

similar observation was reported by Mejri et al, [26] for the CR-Hg^0 complex, where a shift in the oxidation peak for PCR-NS was due to delocalization of electronic charge from the metal complexing site of PCR-NS towards to metal center. This is the evidence for confirming that PCR-NS modified electrode has been highly favored for the preconcentration and complexation with mercury ions present in the electrolyte.

Further study using stripping voltammetry showed the DPASV curves (Fig. 6 **(iii))** for **(a)** bare electrode, **(b)** Hg(II)-bare electrode, **(c)** PCR-NS modified electrode and **(d)** Hg(II)-PCR-NS modified electrode. All the electrodes were scanned by applying differential pulse potential starting from −0.3 to + 0.6 V in 0.1 M NH_4NO_3 electrolyte. A straight line curve with less background current was observed for the bare electrode (**curve (a)**). On preconcentrating the bare electrode with Hg^{2+}, **curve b** showed a peak at potential + 0.2 V corresponding to oxidation of Hg^0. For PCR-NS modified electrode, the DPASV **curve c** exhibited an oxidation peak for PCR-NS at + 0.35 V. Further preconcentrating the PCR-NS electrode with Hg^{2+}, two peaks corresponding to oxidation of Hg^0 and Hg^0-PCR-NS complex were observed at + 0.2 V and + 0.45 V, respectively. A shift in the oxidation peak at + 0.35 V to + 0.45 V was observed due to complex formation between Hg^{2+} and PCR-NS. From the obtained results (Fig. 6 **(i) (ii) & (iii))** it was evident that there is a 10 fold increase in the peak current between unmodified and modified electrodes corresponding to the oxidation of mercury ions. This is due to preconcentration of Hg^{2+} over unmodified electrode occurred due to physisorption, where there is only less concentration of Hg^{2+} accumulated on the unmodified electrode. In the case of PCR-NS modified electrode, the accumulation of $Hg^{2+}$was due to chelation, therefore the concentration of Hg^{2+} is much higher on PCR-NS modified electrode when compared to unmodified electrode resulting in higher oxidation current.

3.5. Parameter optimization

Factors influencing the analytical performance of the PCR-NS modified electrode during stripping analysis of Hg^{2+} were studied.

Table.2
Comparison of previous report with the present work towards determination of Hg^{2+} using DPASV technique.

S. No	Working electrode	Modifier	Metal ion	Concentration range	LOD	Ref
1.	Pencil graphite electrode	4-(4-methylphenyl aminoisonitrosoa- cetyl) biphenyl	Hg^{2+}	1.0×10^{-5} and 1.0×10^{-3} M	5.85×10^{-7} M	39
2.	Carbon paste electrode	Zeolite	Hg^{2+}	0.11 μg/ml–2.2 μg/ml	–	40
3.	Carbon paste electrode	Palladium oxide supported onto natural phosphate (PdO/NP-CPE)	Hg^{2+}	2.5×10^{-7} to 1.0×10^{-4} mol/L	1.93×10^{-8} mol/L	41
4.	Paraffin wax impregnated pencil graphite electrode	Polycurcumin-nanosphere (PCR-NS)	Hg^{2+}	0.21 to 21.72 μ gL^{-1}	70.49 ngL^{-1}	Present work

The effect of background electrolyte, electrolyte pH, and pre-concentration time, were optimized in the presence of Hg^{2+}.

3.5.1. *Effect of background electrolyte*

The basic parameter to be optimized for effective pre-concentration and stripping of Hg^{2+} ions using PCR-NS modified electrode was the selection of suitable background electrolyte solution. The anions and cations present in the background electrolyte may influence the pre-concentration and stripping of Hg^{2+} ions [34]. About 0.1 M concentration of different background electrolyte such as **(a)** $BaCl_2$, **(b)** K_2SO_4, **(c)** KNO_3, **(d)** NaCl, **(e)** $NaNO_3$, **(f)** NH_4Cl, and **(g)** NH_4NO_3 containing 3.9×10^{-6} gL^{-1} of Hg^{2+} ions were taken. The surface of PCR-NS modified electrodes were brought in contact with the metal ion-containing electrolyte solutions and stirred at 500 rpm. The Hg^{2+} pre-concentrated PCR-NS modified electrodes were rinsed in double distilled water and placed in fresh electrolytes for DPASV analysis. The DPASV analysis was carried out at the potential starting from −0.3 to + 0.6 V **(**Fig. 7**.(i)).** Two peaks corresponding to the oxidation of Hg^0 and oxidation of Hg^0-PCR-NS were found at potential + 0.2 V and + 0.45 V, respectively. During DPASV measurement in different electrolyte mediums, the peak appearing for PCR-NS at potential + 0.45 V remained stable with slight changes in the current intensity. The peak at + 0.2 V corresponding to the oxidation of Hg^{2+} was observed in nitrate and sulphate based electrolyte medium. The magnitude of current was higher in nitrate-based electrolytes when compared with sulphate-based electrolytes. In some chloride-based electrolytes, the oxidation potential of mercury was found to be shifted from + 0.2 V to + 0.1 V with a difference in current intensity. Anions such as chloride, hydroxide, can form complex with Hg^0 [41] and could dissociate the preconcentrated Hg^0 from the modified electrode surface to electrolyte which will significantly interfere with the stripping signal. Therefore complexing anion was avoided and nitrate-based electrolytes were chosen as a suitable medium for pre-concentration and stripping of mercury. Among all the nitrate-based electrolytes, 0.1 M NH_4NO_3 solution was chosen as the background electrolyte for the pre-concentration and stripping of Hg^{2+} ions using PCR-NS modified electrode, as the peak, the current intensity was much higher in this electrolyte **(**Fig. 7**.(ii)).**

3.5.2. *Effect of pH*

The composition of the electrolyte medium and pH of the solution equally contributes to Hg^{2+} ion sensing. Concerning pH, the maximum solubility of mercury occurred in all the pH from 1 to 12. By varying the pH of the background electrolyte, preconcentration and stripping conditions of Hg^{2+} ions were optimized. The DPASV analysis was recorded for the Hg^{2+} ion preconcentrated PCR-NS modified electrode by varying the pH of 0.1 M NH_4NO_3 solution from 3.5 to 8.5 using 0.1 M HNO_3 and 0.1 M ammonia water. A graph plot for stripping current versus different pH was plotted and the results are depicted in Fig. 7**.(iii).** It was observed that the decrease in the stripping current at lower pH range 3.5 to 5 was due to electrostatic repulsion between the positively charged Hg^{2+} and PCR-NS modified [42] electrode. At lower pH, the oxidation rate of Hg^0 to Hg^+ and Hg^{2+} was increased, which significantly affect the stripping signal[43]. In pH 5.5, the Hg^{2+} ion competes with the H + ions and is adsorbed on the active sites of the modified electrode. Therefore a maximum stripping current was observed at pH 5.5 which has been fixed as an optimal pH condition for the present experiment. Further increase in the pH range from 6 to 8.5, the adsorption of Hg^{2+} was reduced due to more water-soluble Hg(OH)3- and Hg(OH)4- complex formation [42].

3.5.3. *Effect of pre-concentration time*

The time duration required for the deposition of Hg^{2+} ions over PCR-NS modified electrode is an important parameter to be optimized. The PCR-NS modified electrodes were exposed to Hg^{2+} ions containing 0.1 M NH_4NO_3 solution. The uptake of Hg^{2+} ions by each electrode was measured using DPASV analysis at different time intervals. Fig. 7**.(iv)** shows the dependence of peak current of Hg^{2+} ions on different time intervals. As the exposure time of PCR-NS modified electrodes to Hg^{2+} ion solution increases from 30 to 600 sec, the anodic peak current corresponding to the oxidation of Hg^{2+} also increased. Saturation in the peak current was observed when the exposure time of PCR-NS modified electrode was increased beyond 480 sec. Hence 480 sec was chosen to be the optimal preconcentration time taken by PCR-NS modified electrode for the deposition of Hg^{2+} ions.

3.6. *Determination of Hg^{2+} using DPASV technique*

The DPASV analysis was employed for the determination of Hg^{2+} ions using PCR-NS modified electrode. Under optimal conditions, in 0.1 M NH_4NO_3 solution (pH 5.5), Hg^{2+} ions were added in the concentration range from 0.21 to 21.72 μgL^{-1}. After 480 sec of pre-concentration of Hg^{2+} ions over PCR-NS modified electrode, the electrode underwent a reduction procedure by applying + 0.1 V for 60 sec which was carried out by chronoamperometry technique. During the reduction process, Hg^{2+} ions on the PCR-NS modified electrode were converted into Hg^0. Later DPASV analysis was performed by applying the stripping potential from −0.1 V to 0.8 V. The Hg^0 present on the PCR-NS modified electrode was stripped as Hg^{2+} ions back into the electrolyte solution. During the electrochemical reaction, a peak corresponding to oxidation of Hg^0 was found at + 0.2 V. The DPASV determination of mercury was carried out by increasing the concentration of Hg^{2+} ions, and an anodic shift in the oxidation potential of mercury towards + 0.1 V was found along with the linear increase in peak current. This may be because at a low concentration of Hg, the diffusion is random but at a high concentration, the diffusion process is disrupted which in turn affects the mass transfer. To overcome this issue and to re-establish the mass transfer, more potential was applied to the system [35]. In addition to this reducing current response and cathodic shift in peak, the potential was observed at peak + 0.45 V corresponding to the oxidation of Hg^0-PCR-NS complex. As the concentration of the Hg^{2+} ions increased from 0.21 to 21.72 μgL^{-1}, the peak current for oxidation of PCR decreased with a shift in the potential towards higher voltage as shown in Fig. 8**.(i).** The linear graph was plotted with the concentration of Hg^{2+} ions vs peak current (Fig. 8**.(ii))**, and the regression equation for the calibration plot was found to be i_{pa} 0.35x + 0.550 and the correlation coefficient (r) was found to be 0.99 with the slope value of 0.822nA μgL^{-1} (sensitivity). The developed method showed good linearity for a wide concentration range with the detection limit of 70.49 ngL^{-1}.

3.7. Regeneration of the electrode

After the DPASV measurement of Hg^{2+} ions, the surface of the PCR-NS modified electrode was renewed for the next analysis. But complete removal of Hg^0 ions bound to the electrode surface was not performed during the stripping process. Traces of unstripped Hg^0 was existing at the PCR-NS modified electrode surface. As the electrode was scanned at the potential from −0.4 to + 0.8 V by DPASV, a peak corresponding to the oxidation of Hg^0 was observed at the potential + 0.14 V. The electrode was subjected to a high potential scan from 0 to + 1.2 V. When an increased stripping potential was applied, stable Hg^0-PCR-NS complex gets converted into Hg^{2+}-PCR-NS complex with reduced stability. Then the electrode was dipped in 0.05 M EDTA solution and stirred for 5 min. As EDTA possesses increased affinity towards metal complexation [36], complete dissociation of Hg^{2+} ions from the Hg^{2+}-PCR-NS modified electrode occurred and a pristine PCR-NS modified electrode was obtained for the next measurement. EDTA is a well know chelator and can chelate with most of the heavy metal ions. But due to its water-soluble property, EDTA cannot be directly coated on the electrode surface. There are previous reports where EDTA is bound to polymers, inorganic clays and formed as a composite [44,45]. These composite materials were modified on the electrode surface and used for pre-concentration and stripping analysis of metal ions. In the present study, we utilize EDTA solution for surface regeneration of PCR-NS modified electrode by removing metal ions after stripping procedure.

3.8. Interference study

The development of metal-specific ligand-based electrodes is considered to be promising for metal ion detection. In the previous sections, the analytical method has been developed with suitable optimal conditions for PCR-NS modified electrodes to quantify Hg^{2+} ions with appreciable sensitivity. Interference analysis was carried out to measure the ability of PCR-NS modified electrodes in detecting the stripping signal of Hg^{2+} ions efficiently even in the presence of other species. Under optimized conditions, pre-concentration and stripping procedures for Hg^{2+} ions were carried out in the solution containing K^+, Na^+, Ca^{2+}, Mg^{2+}, Co^{2+}, Cu^{2+}, Pb^{2+}, Zn^{2+}, Cd^{2+} as an interference. All other metal ions, except $Cu^{2+,}$ exhibited different stripping potential when compared with the stripping potential of Hg^{2+} ions. Although the Cu^{2+} ions exhibited stripping potential closer to the stripping potential of Hg^{2+}, the presence of Cu^{2+} ions does not change the signal recorded for Hg^{2+}. Even when the concentration of the other Cu^{2+} ions was increased 100 fold excess compared to the concentration of Hg^{2+} ions, they did not influence the stripping signal of Hg^{2+} ions. The optimized conditions such as electrolyte, pH, and pre-concentration time highly favor the PCR-NS modified electrode to quantify Hg^{2+} ions, specifically.

3.9. Real sample analysis

The analytical parameter optimization for the newly developed PCR-NS modified electrode was successfully applied for the real-time analysis of Hg^{2+} contamination in seawater samples. Fig. 9 showed the DPASV curves for PCR-NS modified electrodes recorded under optimised condition after preconcentration of three replications of 0.1 μgL^{-1} of Hg^{2+} ions (AAS standard) spiked into the seawater samples. A standard protocol widely used for the determination of Hg^{2+} ions present in the water samples is the AAS technique. The most commonly employed absorption line for Hg^{2+} during AAS analysis is at 253.7 nm. Calibration of AAS for Hg^{2+} ions determination was carried out initially with the addition of mercury (0.1 μgL^{-1}) Table. 1 summarizes the results obtained from the developed DPASV method and standard AAS technique. The results obtained from the AAS technique are similar to that of the DPASV technique with AAS showing a recovery percentage of 99.64 % and DPASV of 99.60%.

3.10. Conclusion

In this work, a mercury-free electrode was developed for stripping voltammetry analysis of Hg^{2+} ions using a natural chelating compound, curcumin. Electropolymerization procedure was adopted to prepare nanosphere-shaped polycurcumin film over the graphite electrode. The electrode showed good stability with a current difference of less than 5 % of the base current for the 1st and 100th cycle [37]. Using PCR-NS modified electrode, an analytical method has been developed where the optimal condition is so specific to measure the Hg^{2+} concentration without the interference of other metals. The sensing performance of the modified electrode under optimized conditions was favorable for both high and low concentrations of Hg^{2+} ranging from 0.21 to 21.72 μgL^{-1}. The previous study reported that the determination of Hg^{2+} ions using ligand based chemically modified electrode and the results are compared with the present work (Table 2). In comparison with other modified graphite electrodes [38-40], the developed P

CR-NS modified electrode showed good linearity, high sensitivity (0.8221nA μgL^{-1}), and LOD of 70.49 ngL^{-1}. Amoung other reports, the nanostructure conformation of polycurcumin film boost the sensitivity of PCR-NS electrode towards nanoscale detection of Hg^{2+} ions. The PCR-NS modified electrode can be considered as an alternative to mercury electrodes, exhibiting high efficient and rapid analysis with less pre-concentration time and quick renewable surface for multiple analysis of Hg^{2+} ions. The developed method was successfully applied for seawater analysis. The modified electrode was reused for limited times (20 measurements) without any change in the sensitivity. A fixed concentration of the Hg^{2+} ion was retained and the PCR-NS modified electrode showed 97% of initial current for all the measurements, thus the modified electrode was reproducible. Results obtained by the proposed method for mercury ion detection in the real sample were comparable with the AAS results.

Declaration of Competing Interest

The authors declare that they have no known competing financial interests or personal relationships that could have appeared to influence the work reported in this paper.

Acknowledgment

One of the authors (K. Krishna Kumar) acknowledges the financial support granted from University Grants Commission (UGC), New Delhi under university with potential for excellence (UPE)- Phase II “New Material Research Program”. The author extend his gratitude to Mr. Clavis. V. Lobo, Food safety and content development manager, haccp.com, for his support during language correction.

References

[1] N. Idrees, B. Tabassum, E.F. Abd Allah, A. Hashem, R. Sarah, M. Hashim, Groundwater contamination with cadmium concentrations in some West U.P. Regions, India, Saudi J. Biol. Sci. 25 (2018) 1365–1368. 10.1016/j.sjbs.2018.07.005.
[2] J. Hussain, I. Husain, M. Arif, N. Gupta, Studies on heavy metal contamination in Godavari river basin, Appl. Water Sci. 7 (2017) 4539–4548. 10.1007/s13201-017-0607-4.
[3] W.S. Zhong, T. Ren, L.J. Zhao, Determination of Pb (Lead), Cd (Cadmium), Cr (Chromium), Cu (Copper), and Ni (Nickel) in Chinese tea with high-resolution continuum source graphite furnace atomic absorption spectrometry, J. Food Drug Anal. 24 (2016) 46–55. 10.1016/j.jfda.2015.04.010.
[4] Ö. Tunç Dede, A case study for measurement uncertainty of heavy metal analysis in drinking water with inductively coupled plasma-mass spectrometry (ICP-MS), Anal. Methods. 8 (2016) 5087–5094. 10.1039/c6ay01332e.
[5] D. Han, S.Y. Lim, B.J. Kim, L. Piao, T.D. Chung, Mercury(ii) detection by SERS based on a single gold micro-shell, Chem. Commun. 46 (2010) 5587–5589, https://doi.org/10.1039/c0cc00895h.
[6] A.E. Kandjani, Y.M. Sabri, M. Mohammad-Taheri, V. Bansal, S.K. Bhargava, Detect, remove and reuse: A new paradigm in sensing and removal of Hg (II) from wastewater via SERS-active ZnO/Ag nanoarrays, Environ. Sci. Technol. 49 (2015) 1578–1584, https://doi.org/10.1021/es503527e.

[7] X. Li, G. Chen, L. Yang, Z. Jin, J. Liu, Multifunctional Au-coated TiO2 nanotube arrays as recyclable SERS substrates for multifold organic pollutants detection, Adv. Funct. Mater. 20 (2010) 2815–2824. 10.1002/adfm.201000792.
[8] A. Scozzari, Electrochemical sensing methods: a brief review Andrea Scozzari*, Methods. 335–351 (2008).
[9] J. Buffle, M.L. Tercier-Waeber, Voltammetric environmental trace-metal analysis, and speciation: From laboratory to in situ measurements, TrAC - Trends Anal. Chem. 24 (2005) 172–191. 10.1016/j.trac.2004.11.013.
[10] A.H. Alghamdi, Applications of stripping voltammetric techniques in food analysis, Arab. J. Chem. 3 (2010) 1–7. 10.1016/j.arabjc.2009.12.001.
[11] S.J.R. Prabakar, C. Sakthivel, S.S. Narayanan, Hg(II) immobilized MWCNT graphite electrode for the anodic stripping voltammetric determination of lead and cadmium, Talanta. 85 (2011) 290–297. 10.1016/j.talanta.2011.03.058.
[12] P. Surmann, H. Zeyat, Voltammetric analysis using a self-renewable non-mercury electrode, Anal. Bioanal. Chem. 383 (2005) 1009–1013. 10.1007/s00216-005-0069-7.
[13] J. Wang, B. Tian, Mercury-Free Disposable Lead Sensors Based on Potentiometric Stripping Analysis at Gold-Coated Screen-Printed Electrodes, Anal. Chem. 65 (1993) 1529–1532, https://doi.org/10.1021/ac00059a008.
[14] R. Manikandan, S. Sriman Narayanan, Differential Pulse Anodic Stripping Voltammetric Determination of Lead (II) Using Poly Xylenol Orange Modified Electrode, Electroanalysis. 29 (2017) 609–615. 10.1002/elan.201600368.
[15] J. Jayadevimanoranjitham, S. Sriman Narayanan, A mercury-free electrode based on poly O-cresophthalein complexone film matrixed MWCNTs modified electrode for simultaneous detection of Pb (II) and Cd (II), Microchem. J. 148 (2019) 92–101, https://doi.org/10.1016/j.microc.2019.04.029.
[16] S. Vasanthi, M. Devendiran, S.S. Narayanan, A mercury-free electrode for anodic stripping voltammetric determination of Pb (II) ions using poly zincon film modified electrode, Appl. Surf. Sci. 422 (2017) 138–146, https://doi.org/10.1016/j.apsusc.2017.05.153.
[17] S. Raj, D.R. Shankaran, Curcumin-based biocompatible nanofibers for lead ion detection, Sensors Actuators, B Chem. 226 (2016) 318–325, https://doi.org/10.1016/j.snb.2015.12.006.
[18] S. Wanninger, V. Lorenz, A. Subhan, F.T. Edelmann, Metal complexes of curcumin – synthetic strategies, structures, and medicinal applications, Chem. Soc. Rev. 44 (2015) 4986–5002. 10.1039/C5CS00088B.
[19] S. Wanninger, V. Lorenz, A. Subhan, F.T. Edelmann, Metal complexes of curcumin - synthetic strategies, structures, and medicinal applications, Chem. Soc. Rev. 44 (2015) 4986–5002. 10.1039/c5cs00088b.
[20] A. Ciszewski, G. Milczarek, B. Lewandowska, K. Krutowski, Electrocatalytic Properties of Electropolymerized Ni (II) curcumin Complex, Electroanalysis. 518–523 (2012).
[21] S. Majdi, A. Jabbari, H. Heli, A.A. Moosavi-Movahedi, Electrocatalytic oxidation of some amino acids on a nickel-curcumin complex modified glassy carbon electrode, Electrochim. Acta. 52 (2007) 4622–4629. 10.1016/j.electacta.2007.01.022.
[22] M.Y. Elahi, M.F. Mousavi, S. Ghasemi, Nano-structured Ni(II)-curcumin modified glassy carbon electrode for electrocatalytic oxidation of fructose, Electrochim. Acta. 54 (2008) 490–498. 10.1016/j.electacta.2008.07.042.
[23] R. Ojani, J.B. Raoof, S. Zamani, A novel voltammetric sensor for amoxicillin based on nickel-curcumin complex modified carbon paste electrode, Bioelectrochemistry. 85 (2012) 44–49, https://doi.org/10.1016/j.bioelechem.2011.11.010.
[24] K.K. Kumar, M. Devendiran, R.A. Kalaivani, S.S. Narayanan, Enhanced electrochemical sensing of dopamine in the presence of AA and UA using curcumin functionalized gold nanoparticle modified electrode, New J. Chem. 43 (2019) 19003–19013, https://doi.org/10.1039/c9nj04398e.
[25] N. Pourreza, H. Golmohammadi, S. Rastegarzadeh, Highly selective and portable chemosensor for mercury determination in water samples using curcumin nanoparticles in a paper-based analytical device, RSC Adv. 6 (2016) 69060–69066. 10.1039/c6ra08879a.
[26] A. Mejri, A. Mars, H. Elfil, A.H. Hamzaoui, Graphene nanosheets modified with curcumin-decorated manganese dioxide for ultrasensitive potentiometric sensing of mercury (II), fluoride and cyanide, 2 (2018) 3–10.
[27] A. Mars, M. Hamami, L. Bechnak, D. Patra, N. Raouafi, Graphical abstract SC, Anal. Chim. Acta. (2018), https://doi.org/10.1016/j.aca.2018.06.075.
[28] K.M. Mohibul Kabir, D. Jampaiah, A.E. Kandjani, M. Mullett, J. Tardio, Y.M. Sabri, S.K. Bhargava, Cold vapor integrated quartz crystal microbalance (CV-QCM) based detection of mercury ions with gold nanostructures, Sensors Actuators, B Chem. 290 (2019) 453–458. 10.1016/j.snb.2019.04.022.
[29] B. Devadas, M. Rajkumar, S.M. Chen, Electropolymerization of curcumin on glassy carbon electrode and its electrocatalytic application for the voltammetric determination of epinephrine and p-acetoaminophenol, Colloids Surfaces B Biointerfaces. 116 (2014) 674–680, https://doi.org/10.1016/j.colsurfb.2013.11.002.
[30] F. Scholz, B. Lange, Abrasive stripping voltammetry - electrochemical solid state spectroscopy of wide applicability, Trends Anal. Chem. 11 (1992) 359–367, https://doi.org/10.1016/0165-9936(92)80025-2.
[31] J.B. Raoof, R. Ojani, M. Kolbadinezhad, Electrocatalytic characteristics of ferrocene carboxylic acid modified carbon paste electrode in the oxidation and determination of L-cysteine, Electroanalysis. 17 (2005) 2043–2051. 10.1002/elan.200403332.
[32] V.T. Bich, N.T. Thuy, N.T. Binh, N.T.M. Huong, P.N.D. Yen, T.T. Luong, Structural and spectral properties of curcumin and metal- curcumin complex derived from turmeric (Curcuma longa), Springer Proc. Phys. 127 (2009) 271–278. 10.1007/978-3-540-88201-5_31.
[33] M.M. Yallapu, M. Jaggi, S.C. Chauhan, β-Cyclodextrin-curcumin self-assembly enhances curcumin delivery in prostate cancer cells, Colloids Surfaces B Biointerfaces. 79 (1) (2010) 113–125, https://doi.org/10.1016/j.colsurfb.2010.03.039.
[34] L.H. Marcolino-Junior, B.C. Janegitz, B.C. Lourenção, O. Fatibello-Filho, Anodic stripping voltammetric determination of mercury in water using a chitosan-modified carbon paste electrode, Anal. Lett. 40 (2007) 3119–3128. 10.1080/00032710701645463.
[35] Borrill, A., Reily, N. E., & Macpherson, J. V. (2019). Addressing the Practicalities of Anodic Stripping Voltammetry for Heavy Metal Detection: A Tutorial Review. The Analyst. 10.1039/c9an01437c.
[36] P. Liu, T. Yan, J. Zhang, L. Shi, D. Zhang, Separation and recovery of heavy metal ions and salt ions from wastewater by 3D graphene-based asymmetric electrodes: Via capacitive deionization, J. Mater. Chem. A. 5 (2017) 14748–14757. 10.1039/c7ta03515b.
[37] A. Kalaivani, S. Sriman Narayanan, A novel electrochemical immobilization of Hg in CdSe QDs - modified graphite electrode and its improved performance in voltammetric determination of lead (II) ion, Mater. Today Proc. (2020) 8–11. 10.1016/j.matpr.2020.07.019.
[38] S. Percin Ozkorucuklu, G. Yildirim, T. Sardohan Koseoglu, F. Karipcin, E. Kir, Voltammetric determination of mercury (II) using a modified pencil graphite electrode with 4-(4-methyl phenyl aminoisonitrosoacetyl)biphenyl, J IRAN CHEM SOC 14 (8) (2017) 1651–1657.
[39] P. Hernández, E. Alda, L. Hernández, Determination of mercury (II) using a modified electrode with zeolite, Z. Anal. Chem. 327 (1987) 676–678.
[40] F. El Aroui, S. Lahrich, A. Farahi, M. Achak, L. El Gaini, B. Manoun, M. Bakasse, A. Bouzidi, M.A. El Mhammedi, Electrochemical determination of mercury (II) in ambient water at palladium oxide/graphite composite electrodes, Journal of the Taiwan Institute of Chemical Engineers 45 (5) (2014) 2725–2732.
[41] M. Ravichandran, Interactions between mercury and dissolved organic matter - a review, Chemosphere 55 (2004) page 323.
[42] Hamideh Khademzadeh Moghaddam, Majid Pakizeh, Experimental study on mercury ions removal from aqueous solution by MnO2/CNTs nanocomposite adsorbent, Journal of Industrial and Engineering Chemistry 21 (2015) 221–229.
[43] M.C. Canela, W.F. Jardim, The Fate of Hg0 in Natural Waters, J. Braz. Chem. Soc. 8 (4) (1997) 421–426.
[44] M.A. Rahman, M.S. Won, Y.B. Shim, Characterization of an EDTA bonded conducting polymer modified electrode: its application for the simultaneous determination of heavy metal ions, Anal Chem 75 (2003) 1123–1129.
[45] J. Dong, Q. Fang, H. He, Y. Zhang, J. Xu, Y. Sun, Electrochemical sensor based on EDTA intercalated into layered double hydroxides of magnesium and aluminum for ultra-trace level detection of lead (II), Microchim Acta 182 (3-4) (2015) 653–659.